Commonwealth Marine Economies Programme

Enabling safe and sustainable marine economies across Commonwealth Small Island Developing States

www.cmeprogramme.org | CME.ProgrammeEnquiries@fco.gov.uk

Funded by UK Government

PACIFIC MARINE CLIMATE CHANGE REPORT CARD
Science Review 2018: *pp* 20-30

Effects of Climate Change on Sea Temperature Relevant to the Pacific Islands

Philip J H Sutton, National Institute of Water and Atmospheric Research (NIWA), New Zealand, and University of Auckland, New Zealand.

EXECUTIVE SUMMARY

The average ocean temperature field in the western tropical Pacific is a result of a combination of differential heating between the equator and higher latitudes together with local and remote wind forcing driving warm surface water to the west to form the Warm Pool where sea surface temperature (SSTs) near 30°C. SSTs above 27-28°C are associated with strong atmospheric convection, limiting further SST increase and resulting in high rainfall. The atmospheric convection makes the Warm Pool a critical part of the atmospheric Walker circulation, which in turn maintains the trade winds. Ocean temperatures in the western tropical Pacific are highly variable, largely as a result of El Niño/Southern Oscillation (ENSO) and Interdecadal Pacific Oscillation (IPO) changes. Observations indicate that the western tropical Pacific has warmed, although the precise pattern of warming is hard to define against the strong background variability. There is a clearer signal in the expansion of the Warm Pool area. Model projections indicate that the warming and Warm Pool expansion will both continue into the future, with significant impacts on rainfall and ocean stratification.

Introduction

This work examines the past changes in sea surface temperature (SST) in the region between 25N and 25S, 120E to 240E, that is, the western tropical Pacific. Globally, the ocean has absorbed more than 90% of the additional heat due to recent global warming because of the high heat capacity of water (Rhein *et al*, 2013). This warming has resulted in a globally averaged SST increase of ~0.67°C from 1901 to 2005, a warming rate of 0.06°C/decade. SSTs in the western tropical Pacific have warmed by as much as 1 to 1.5°C in the past 50 years (Cravatte *et al*., 2009).

The SST of the tropical Pacific varies both spatially and temporally. More heat is absorbed by the ocean near the equator that at higher latitudes, resulting in a background pattern of cooling away from the equator towards the poles. On top of this background gradient, SST depends on a broad range of processes including diurnal and seasonal changes, air-sea heat exchanges, horizontal ocean heat transport by currents and eddies and vertical ocean heat transport by upwelling and mixing.

Centre for Environment Fisheries & Aquaculture Science

United Kingdom Hydrographic Office

National Oceanography Centre
NATURAL ENVIRONMENT RESEARCH COUNCIL

The western tropical Pacific is an oceanographically complicated region. There are westward currents at ~18°N and 3°S called the North and South Equatorial Currents respectively, mainly driven by the easterly trade winds. In contrast, there are eastward currents at ~5°N and 8°S: respectively, the North and South Equatorial Counter Currents. The flows south of the equator are further complicated by interactions with island chains and land masses. A current schematic can be found in Ganachaud *et al*. (2011). The trade winds and resultant westward ocean currents effectively push warm equatorial surface water into the western tropical Pacific, maintaining a warm volume of water called the 'Warm Pool' with surface temperatures nearing 30°C. The prevailing winds also cause equatorial upwelling, and coastal upwelling along the coast of South America, both of which bring relatively cool, nutrient rich water to the surface. This results in a tongue of cooler water extending along the equator from the South American coast to the central Pacific, where it meets the eastern limit of the Warm Pool at around 180-220°E.

There is an effective upper limit of SST. Once SST reaches 27-28°C, atmospheric convection occurs, limiting further SST increases by removing heat from the ocean (e.g. Waliser and Graham, 1993). The result of this mechanism is that tropical SSTs are limited to about 32°C (e.g., Tompkins, 2001).

This area is strongly linked to the El Niño/Southern Oscillation (ENSO) system. Under normal conditions, the Warm Pool provides a large heat reservoir which maintains the atmospheric Walker circulation, and therefore the trade winds, in a positive feedback loop. In El Niño conditions the trade winds weaken and the warm pool spreads east taking its associated precipitation and wind events with it. At the end of El Niño, the system can 'overshoot' to enter a period of more extreme trade winds with the Warm Pool being more strongly confined to the western side of the Pacific basin - this is La Niña. ENSO is irregular, but typically has a quasi 4-year cycle and dominates decadal variability.

On longer time scales there is variability related to the Interdecadal Pacific Oscillation (IPO). The IPO is similar to ENSO, but spans multidecadal timescales. The SST patterns associated with the IPO are similar to those of ENSO, although the pattern extends further away from the equator, and the oscillation between positive and negative phases can take decades, rather than a few seasons. The existence of multi-decadal natural variability complicates the calculation and interpretation of trends in ocean temperatures by making it difficult to discriminate trends from natural variability.

Two sea surface temperature (SST) products are used in this analysis. The first is a reconstructed sea surface temperature (NOAA Extended Reconstructed Sea Surface Temperature: ERSST.v5) provided by NOAA and available via http://www.esrl.noaa.gov/psd/. This product has 2° latitude and longitude spatial resolution and monthly temporal resolution extending back to 1854 (Huang *et al*., 2017). The second is an objectively-analysed SST product based on satellite measurements, also provided by NOAA (NOAA OI SST V2 High Resolution Dataset). These data are higher resolution, with 0.25° latitude and longitude spatial resolution and daily temporal resolution but are only available for the period since September 1981 when the AVHRR satellite measurements began (Reynolds *et al*., 2007).

It should be noted that prior to the satellite measurements beginning in 1981 there were very few measurements in the region and so the extended reconstructed SST (ERSST) should be interpreted cautiously for the early period.

What is Already Happening?

a) Timeseries at selected sites.

SST timeseries were extracted from the ERSST and OI-daily-SST products for the locations shown in Figure 1. These locations were chosen to be near capital cities with extra sites added to cover the region.

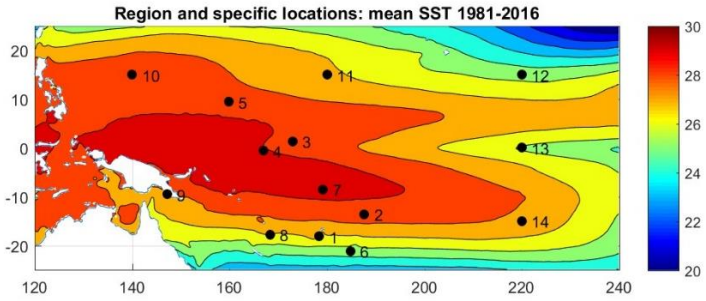

Figure 1. The study region. Specific sites are shown by the black dots. The background is the mean SST between 1981 and 2016 calculated from the OI-daily-SST product.

The individual timeseries are shown in Figure 2.1 – 2.14. In each plot, the light grey line shows the SST at the full ERSST resolution, that is monthly. The black line is the same timeseries annually smoothed – thereby removing the annual cycle. The red line after 1981 is the annually-smoothed OI-daily-SST averaged over a 1°latitude/longitude area centred on the location. The ERSST and OI-daily-SST results are

consistent, but the OI-daily has much higher variability. The differences in variability in the grey curves between sites are largely caused by the amplitude of the annual cycle and hence are a reflection of how far the site is from the equator. All of the timeseries show significant decadal variability, and some indicate a warming trend in the modern satellite era. This will be discussed later.

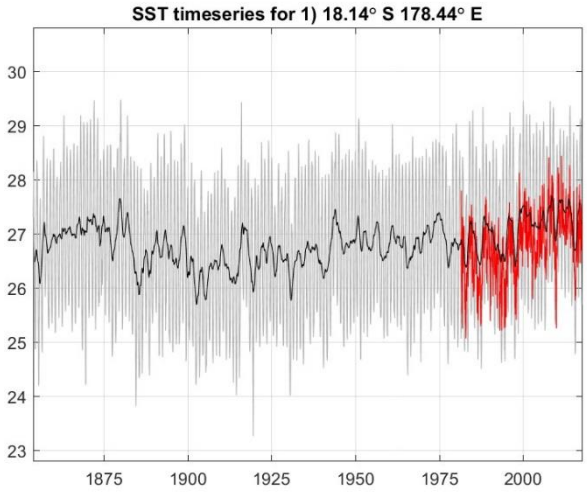

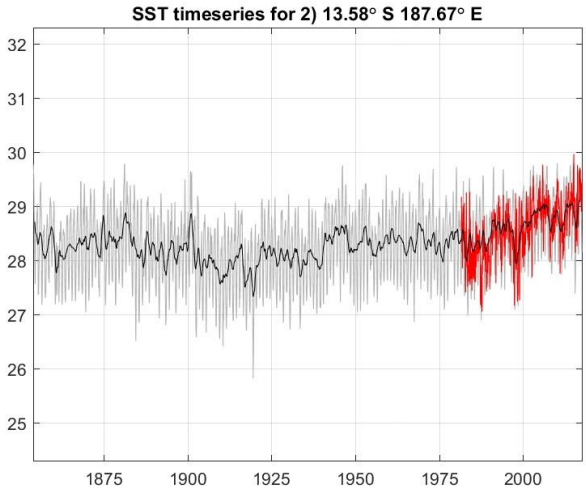

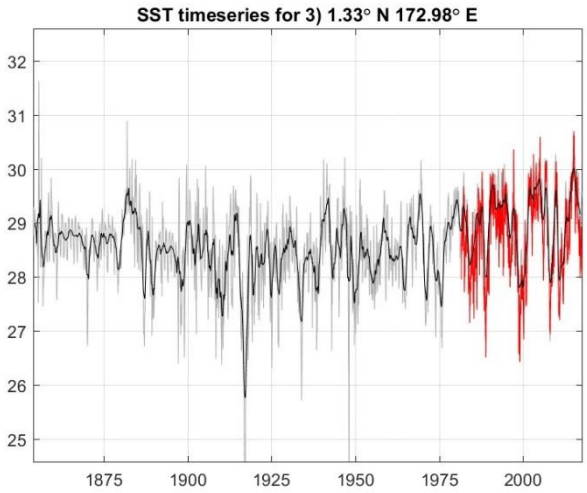

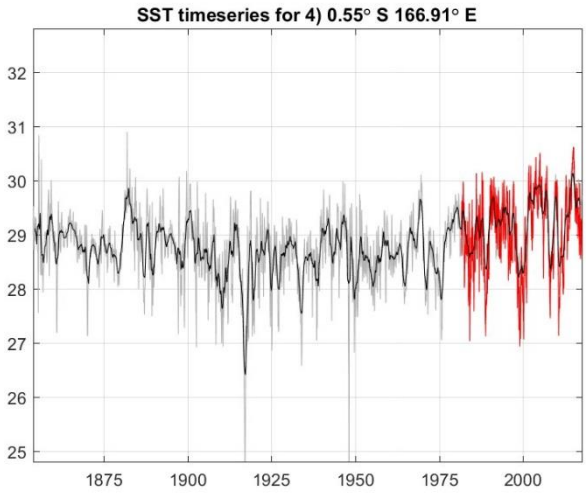

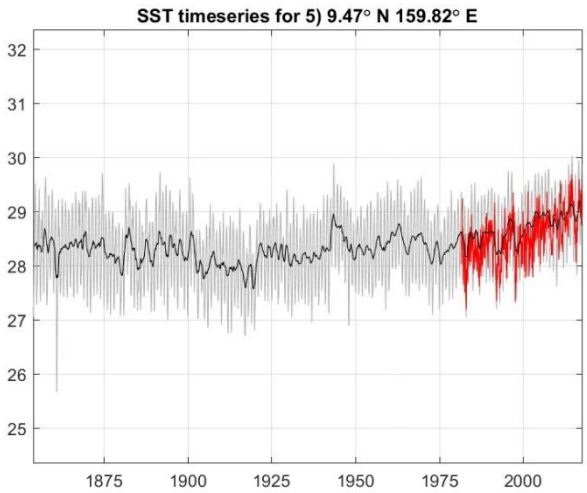

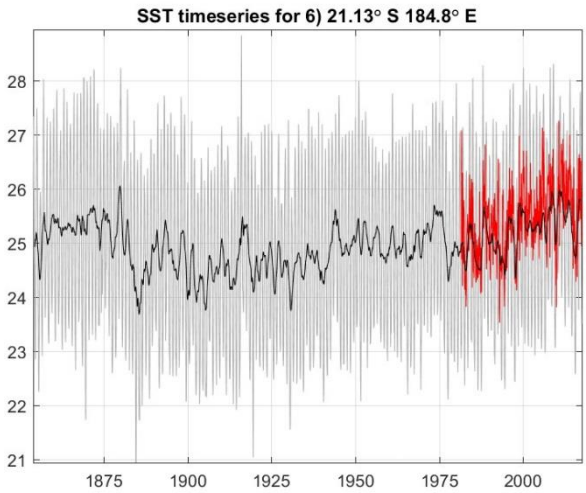

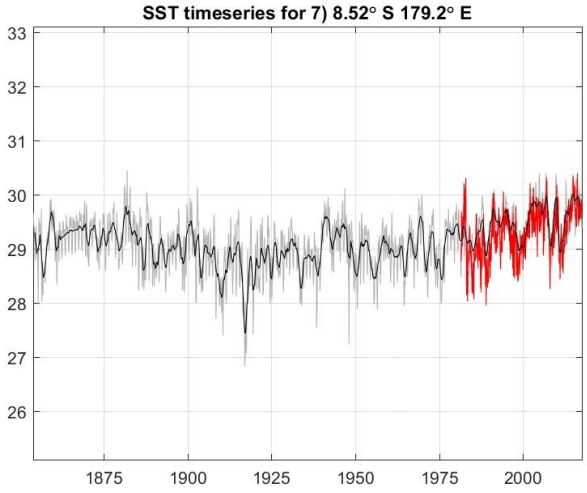
SST timeseries for 7) 8.52° S 179.2° E
33
32
31
30
29
28
27
26
1875
1900
1925
1950
1975
2000

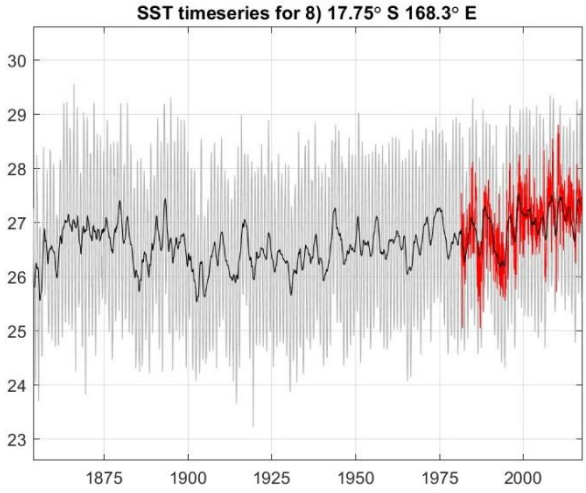
SST timeseries for 8) 17.75° S 168.3° E
30
29
28
27
26
25
24
23
1875
1900
1925
1950
1975
2000

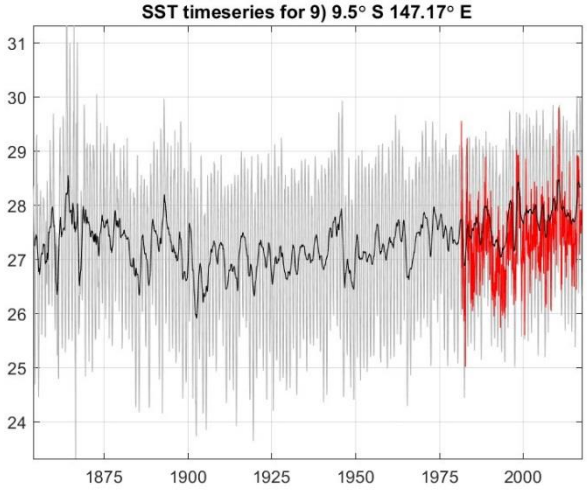
SST timeseries for 9) 9.5° S 147.17° E
31
30
29
28
27
26
25
24
1875
1900
1925
1950
1975
2000

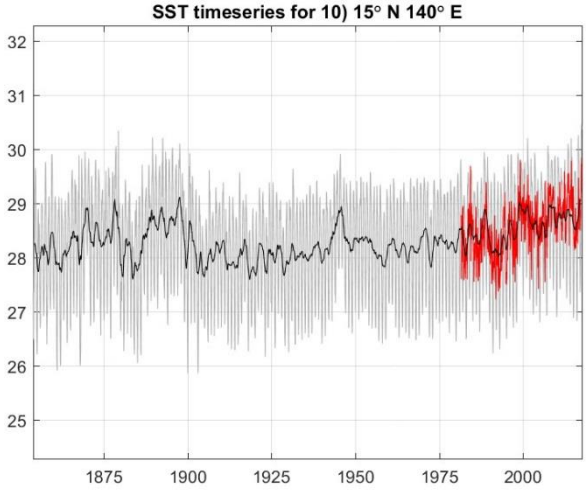
SST timeseries for 10) 15° N 140° E
32
31
30
29
28
27
26
25
1875
1900
1925
1950
1975
2000

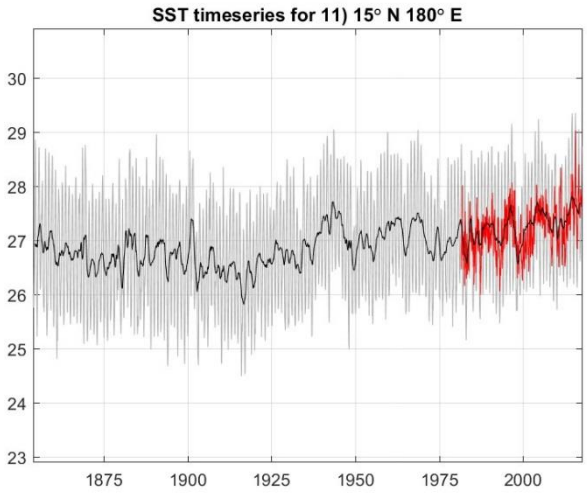
SST timeseries for 11) 15° N 180° E
30
29
28
27
26
25
24
23
1875
1900
1925
1950
1975
2000

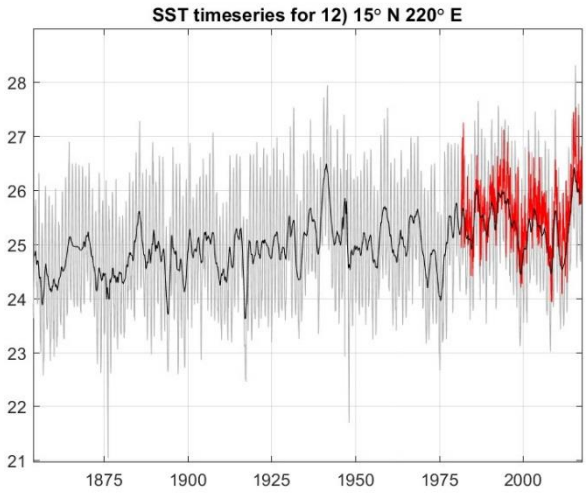
SST timeseries for 12) 15° N 220° E
28
27
26
25
24
23
22
21
1875
1900
1925
1950
1975
2000

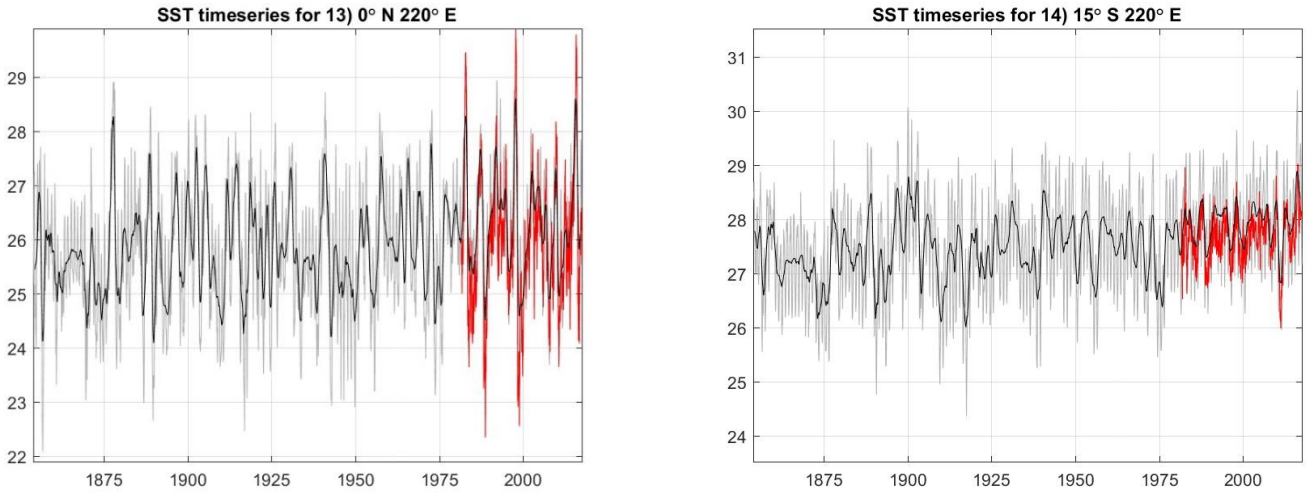

Figure 2. The individual timeseries for the locations in Figure 1 are shown in Figure 2.1 – 2.14. Light grey: SST at the full (monthly) ERSST resolution. Black: ERSST timeseries annually smoothed. Red: annually-smoothed OI-daily-SST averaged over a 1°latitude/longitude area centred on the location.

b) Seasons

Seasonal changes are relatively weak in the region because it is near the equator. The mean monthly SSTs were calculated from the daily-OI-SST product and are shown in Figure 3. The seasonal cycle is evident as the Warm Pool moving south in Austral summer and north in Boreal summer, with the seasonal peaks occurring around February and August.

c) El Niño/Southern Oscillation

As stated earlier, ENSO has a strong impact on the region, with El Niño periods corresponding to an eastward movement of the Warm Pool as the trade winds weaken and La Niña a westward concentration of the warm pool as trade winds strengthen. There are a number of indices used to describe ENSO (e.g., Hanley *et al*., 2003), with two of the most commonly used being the Southern Oscillation Index (SOI) and Niño-3.4. The SOI measures the atmospheric pressure difference between Tahiti and Darwin, and is therefore a measure of trade wind strength in the western Pacific. Negative values of the SOI correspond to El Niño conditions while positive SOI values coincide with La Niña events. Niño-3.4 is based on SST anomalies across an area of ocean bordered by 5°N-5°S and 170°E to 240°E. The SOI has been used in this study because the Niño-3.4 definition overlaps the study region and so high correspondence would have been inevitable.

Figure 4 shows the correlations between the annually-smoothed SST and SOI, both for the full ERSST time period and for the shorter period overlapping with the satellite data period since 1981. The annual smoothing was done to focus the analysis on interannual variability.

The strong correlations, both positive and negative, confirm that ENSO is a dominant forcing mechanism for interannual SST variability in the study region. To highlight the correspondence, timeseries of SST and SOI are shown for two locations in Figure 5. The first location (location 13 in Figure 2) is on the equator in the region of high negative correlation. Figure 2.13 shows the highest variability of the timeseries from specific sites in Figure 2, and is also notable because the variability is predominantly interannual – that is, the annually-smoothed timeseries has comparable variability to the monthly timeseries. This high interannual variability is a result of ENSO variability: location 13 is on the eastern edge of the mean Warm Pool and so is highly impacted by the westward and eastward movements of the warm Pool in response to ENSO forcing. The second is in the southern area of significant positive correlation.

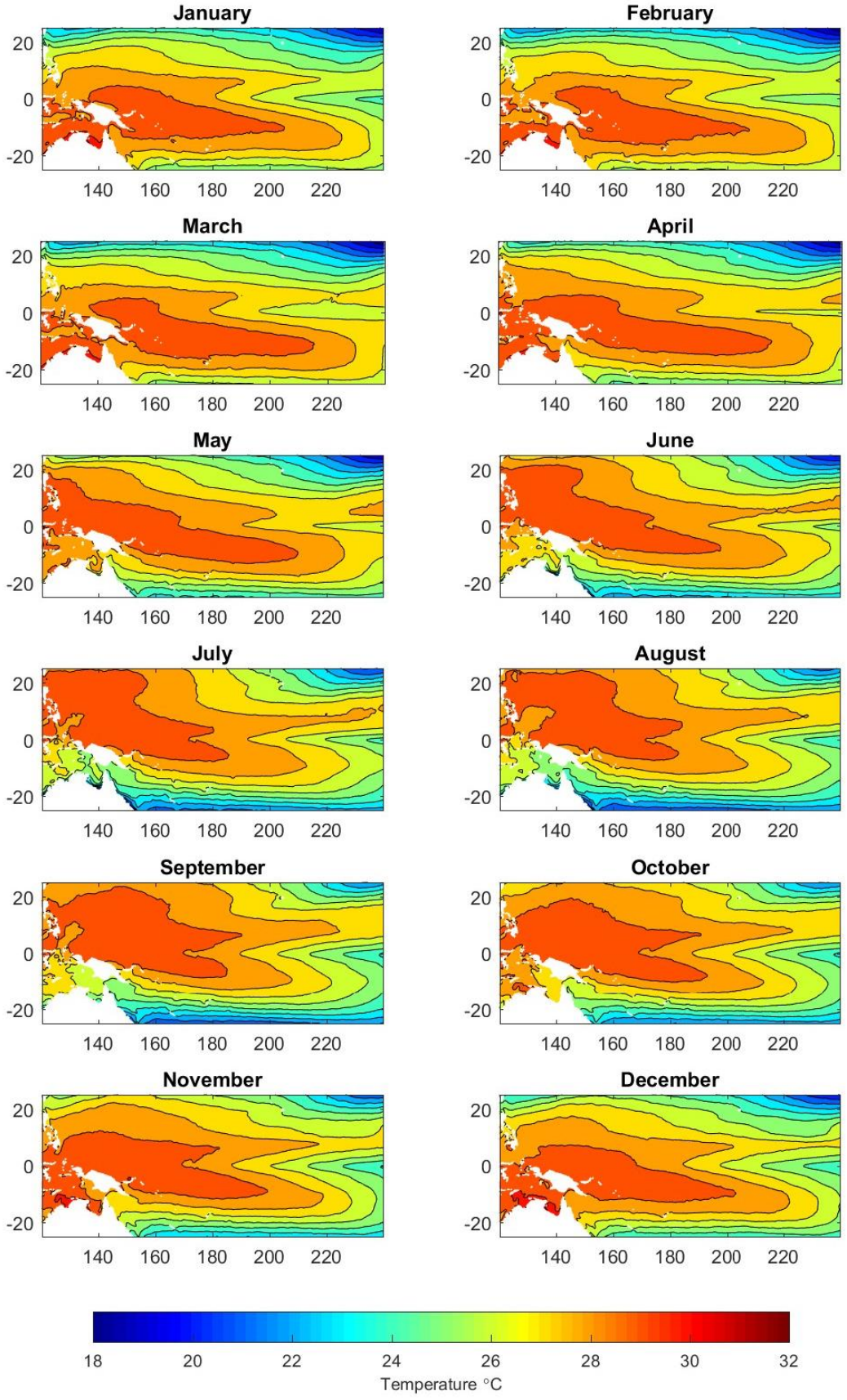

Figure 3. Monthly mean SSTs calculated from OI-daily-SST (between 1981 and 2016).

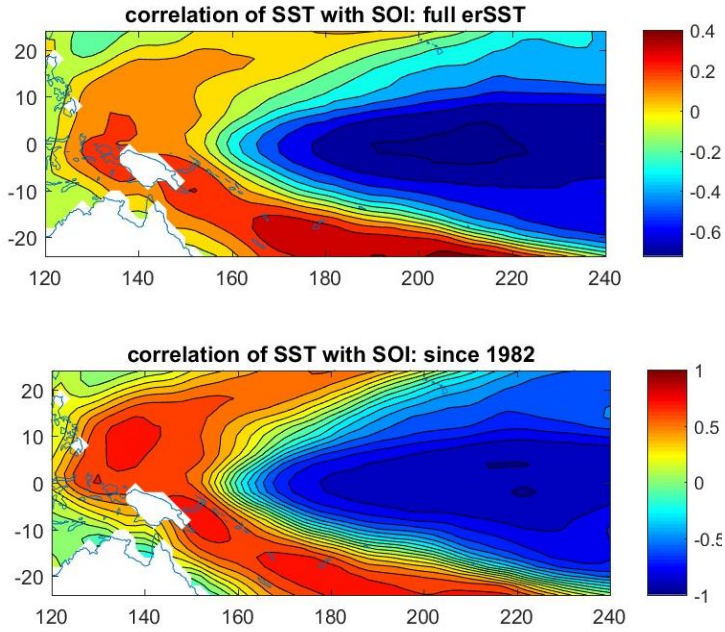

Figure 4. The correlations between the annually-smoothed ERSST and SOI, both for the full ERSST time period (top) and for the shorter period overlapping with the satellite data period since 1981 (bottom).

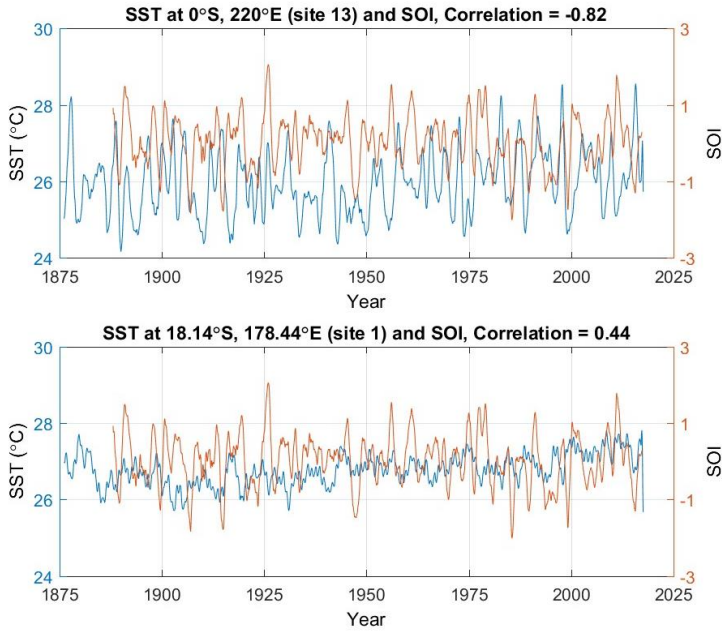

Figure 5. Annually-smoothed SST (blue) and SOI (red) for two locations with strong negative and positive correlations.

d) Trend

While it is possible to calculate linear trends over various periods, it is difficult to know how to interpret them. This is because the results are very sensitive to the time periods chosen, largely because of the strong decadal variability resulting from ENSO. An obvious first choice is to calculate the trend over the modern satellite period where the data are high quality. To do this, the OI-daily-SST was first deseasoned by subtracting the mean seasonal cycle calculated over the 35 year timeseries at each location. It was then smoothed with a one year running mean filter to remove high frequency variability. Finally, the linear trend over the period since 1981 was calculated by fitting a straight line to the timeseries at each location. The linear trends in SST are shown in Figure 6a) in units of °C/decade. The spatial pattern of this result resembles ENSO variability, and indeed, over the 1981 to present period there was been a trend in the SOI. Nonetheless, since 1981 there has been a small warming of ~0.1°C/decade along the equator in the Warm Pool region. Regions of stronger warming occur to the north and south of the Warm Pool, with the highest trend of ~0.3°C/decade at ~12°S, 185°E. The eastern end of the study region shows a cooling trend since 1981, with peak cooling rates of ~-0.15°C/decade at ~10°S and ~25°N, 240°E.

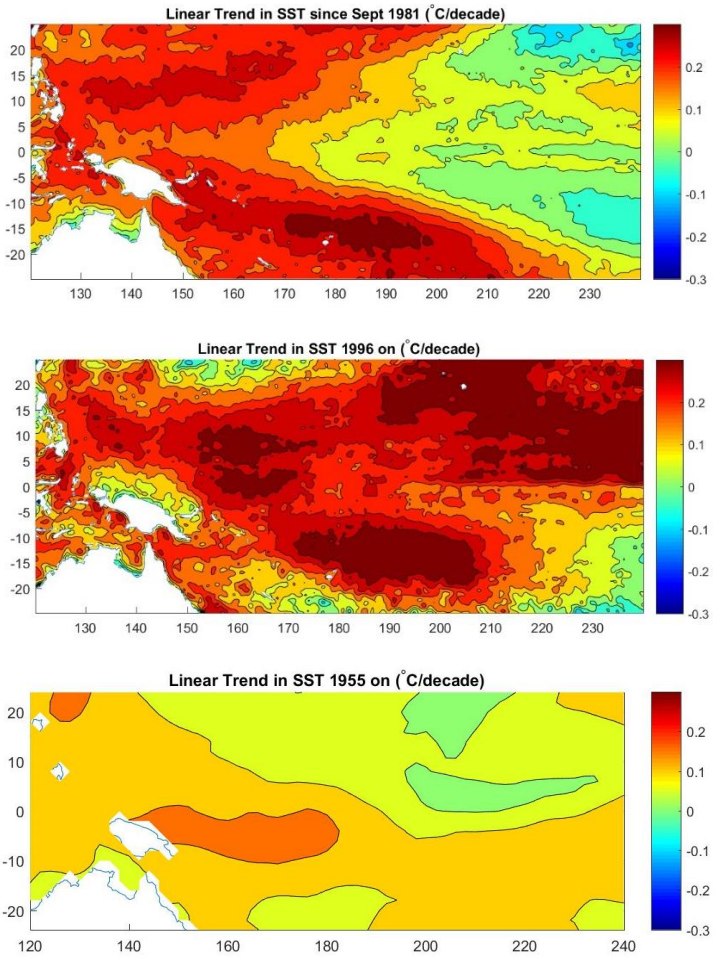

Figure 6. a) and b) Linear trends in SST calculated from the annually-smoothed, deseasoned OI-daily-SST over the time periods September 1981 on (a) and 1996 on (b). c) The linear trend in SST calculated from the annually-smoothed ERSST product for the period from 1955 on.

Two other attempts to estimate warming rates that are not impacted by ENSO variability were made. The first

was to calculate a trend as above, but only based on the period 1996 on, over which there was no significant trend in the SOI. This is a noisier result, being based on a shorter time span. It shows warming of up to 0.3°C/decade over much of the study domain. Finally, the analysis was repeated using the ERSST product to examine change since 1955, which was suggested as a starting point for trend analysis by Cravatte *et al*. (2009). The ERSST product has lower spatial resolution and the trends are smaller over the longer time period, but still indicate a warming of up to 0.1°C/decade over much of the domain.

In summary, all of these trend analyses indicate warming, but defining exact decadal change is impossible given the strong decadal variability associated with ENSO.

The patterns in the warming trends are partially a result of the equatorial water already being near the upper limit of ~32°C (e.g., Tompkins, 2001). Once the SST is above ~27°C, strong atmospheric convection occurs, removing heat from the ocean and reducing further SST increase. Of course, the atmospheric convection has strong impacts on local winds and rainfall. This upper limit means that further warming of the Warm Pool is limited. What has occurred is an expansion of the Warm Pool – Figure 7 a) shows the position of the 29°C contour for the means of two five-year time periods: 1982-1986 at the beginning of the satellite era and the most recent period of 2012-2017.

This expansion of the Warm Pool is a dramatic signal that accounts for the strong warming trends in Figure 6a) and 6b) at the southern and northern margins of the Warm Pool as it expands. The curves in Figure 7b) indicate that the expansion of the Warm Pool is not an artefact of ENSO variability - while the area has not increased monotonically, there is a clear signal of increase since 1981.

What Could Happen?

Simulating the projected features of the Warm Pool is a major challenge for numerical models due to difficulties in realistically simulating SST, precipitation and salinity. Nonetheless, climate models consistently indicate that warming and freshening will continue (Australian Bureau of Meteorology and CSIRO, 2011), with projected 100 year warming of the order of 1 to 3°C and freshening of 0.2 to 0.34 PSU (practical salinity unit: 1 PSU = 1 g per kg of sea water) depending on the climate scenario (e.g. Figure 8). The difference in projected sea surface salinity changes across the models is considerably larger than for SST, in part due to large inter-model differences in the representation of mean rainfall.

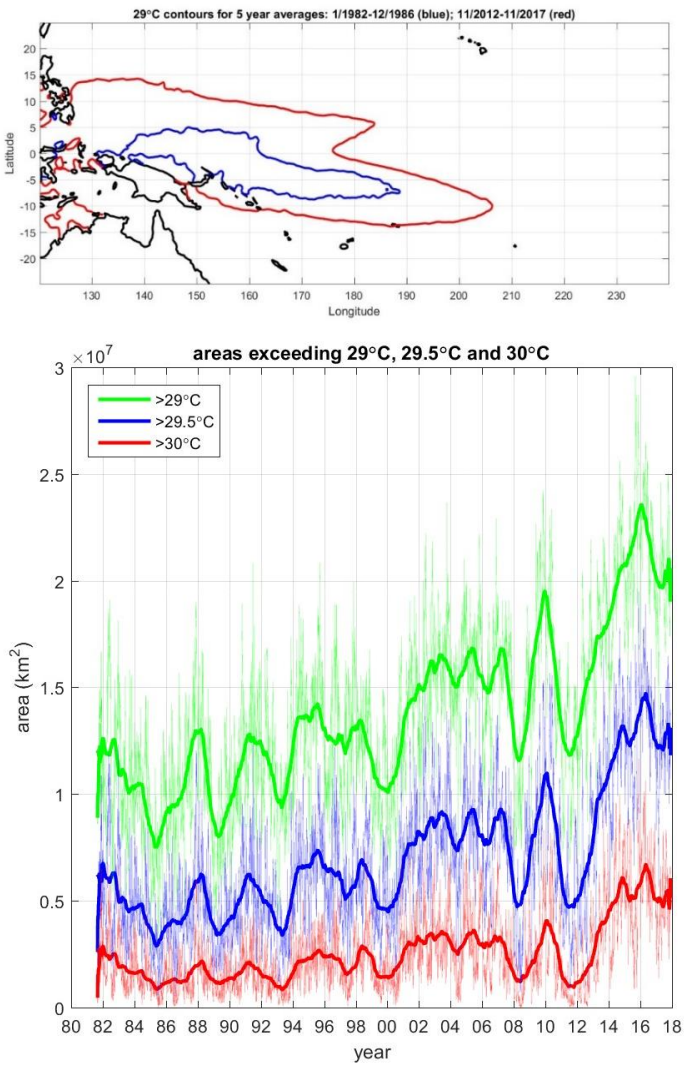

Figure 7. a) The 29°C contour for the mean over two five-year time periods: 1982-1986 at the beginning of the satellite era in blue and the most recent period, 2012-2017 in red. b) The area bounded by the 29°C, 19.5°C and 30°C contours since 1981 (at daily resolution and annually-smoothed).

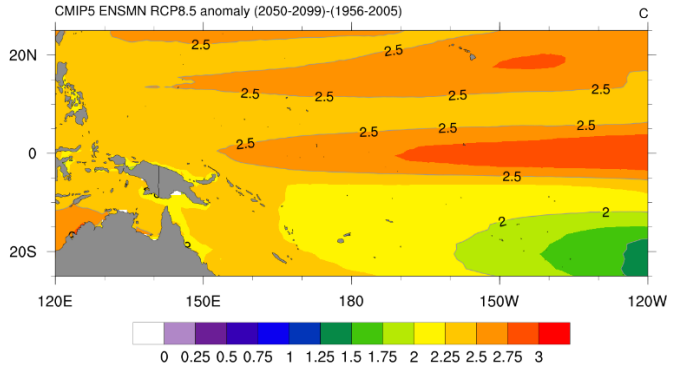

Figure 8. The projected change in sea surface temperature from an average of 1956-2005, to 2050-2099, under a high emissions scenario (RCP 8.5). From NOAA Climate Change Portal. https://www.esrl.noaa.gov/psd/ipcc/ocn/.

Many climate models indicate maximum warming in the central equatorial Pacific (e.g. Figure 8). The salinity changes are due to increased rainfall vs evaporation resulting from increased atmospheric convection over warmer water. The Warm Pool is projected to enlarge massively into the future in a continuation of the signal seen since the 1980s (Figure 7). This could result in the area of convection and high rainfall increasing in unison, although there are model results that indicate that the convective SST threshold will increase in the future so that the area of strong convection and therefore surface freshening will not expand as much as the Warm Pool (Johnson and Xie, 2010). Nonetheless, the salinity front at the equator is projected to move east by ~1400km by 2100 under moderate warming scenarios.

The surface warming and increased rainfall have several ramifications. One is that the ocean becomes more strongly stratified because warm, fresh water is less dense than cold, salty water. Increased stratification is postulated to have an effect on biological productivity by lowering the mixing of nutrients from the deeper ocean up into the shallow euphotic zone (Ganachaud *et al*., 2011, Bell *et al*., 2011). There are likely to be many other biological impacts, in particular on fisheries and coral bleaching (e.g., Doney *et al*., 2005). Increased stratification could also serve to exacerbate further warming by creating a thinner surface layer to absorb incoming solar radiation. A further theoretical result of surface warming and freshening is a weakening of the atmospheric circulation, including the trade winds (Held and Soden, 2006). Model simulations indicate corresponding decreases in the westward-flowing North and South equatorial currents. Changes in the trade winds and equatorial currents will change the local conditions and impact on ENSO structure and variability, which dominates the interannual variability throughout the region. Currently, climate models don't provide consistent projections for any changes in the frequency, intensity and structures of future ENSO events. Similarly, it is possible that the nature of the Interdecadal Pacific Oscillation will change in the future, but there is no knowledge of how this may be manifested.

It is thought that a warmer ocean could lead to more or stronger tropical cyclones. To date there have been no significant trends in either the frequency or intensity of tropical cyclones. However, the observation period is still relatively short to analyse erratic events like tropical cyclones.

An indirect impact of a warming ocean is rising sea level - warm water is less dense and so stands taller. Between a third and a half of global sea level rise has been attributed to ocean warming.

Confidence Assessment

What is already happening

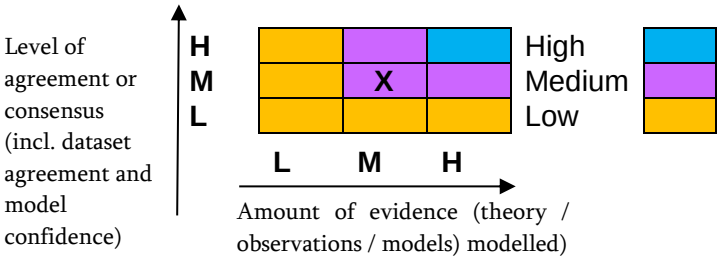

What could happen in the future

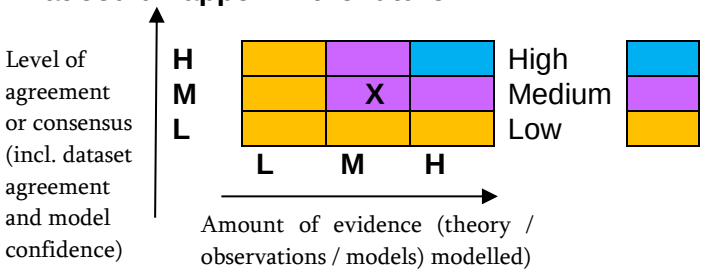

There is generally a high level of consensus and evidence for what is already happening and what could happen in the future. What holds the assessments at 'medium' are the uncertainties caused by the high degree of innate variability due to ENSO and the IPO. There is also uncertainty about how the Warm Pool and the heat loss mechanism through atmospheric convection will evolve into the future.

Knowledge Gaps

1) It is very difficult to separate trends from variability in this region because of strong interannual variability from ENSO and multi-decadal variability from the IPO. Ultimately this will only be solved by having sufficiently long and accurate measurements.
2) This work has solely focussed on SST, but the subsurface ocean is also variable and key to processes in the area. Argo, an international programme maintaining a global network of profiling floats, has been measuring the upper 2000m of the ocean globally since 2004. There have also been measurement campaigns along the equator from moorings targeting

ENSO processes Tropical Moored Buoy System- TOGA). It is critical that these measurements are maintained into the future so that the full ocean impacts of climate change can be ascertained.

3) In parallel with the improving data are improving models with higher resolution and more accurately-represented processes. Finally, there is the opportunity to couple the measurements and the models in data assimilating models or ocean state estimates. This evolution in capability will enlighten the changes taking place.

Acknowledgements

NOAA_ERSST_V5 and NOAA High Resolution SST data were provided by the NOAA/OAR/ESRL PSD, Boulder, Colorado, USA, from their website at http://www.esrl.noaa.gov/psd/.

Citation

Please cite this document as:

Sutton, P.J.H. (2018) Impacts of Climate Change on Sea Temperature Relevant to the Pacific Islands. Pacific Marine Climate Change Report Card: Science Review 2018, pp 20-30.

The views expressed in this review paper do not represent the Commonwealth Marine Economies Programme, individual partner organisations or the Foreign and Commonwealth Office.

References

Australian Bureau of Meteorology and CSIRO, (2011) Climate Change in the Pacific: Scientific Assessment and New Research. Volume 1: Regional Overview. www.pacificclimatechangescience.org.

Bell, J.D., Johnson, J.E. and Hobday, A.J. (eds.) (2011) *Vulnerability of Tropical Pacific Fisheries and Aquaculture to Climate Change*. Secretariat of the Pacific Community (SPC), Noumea, New Caledonia.

Chen J.Y., Del Genio, A.D., Carlson, B.E., and Bosilovich, M.G. (2008) The spatiotemporal structure of twentieth-century climate variations in observations and reanalyses. Part I: Long-term trend. *Journal of Climate* 21, 2611–2633.

Cravatte S, Delcroix, T., Zhang, D., McPhaden, M. and Leloup, J. (2009) Observed freshening and warming of the western Pacific warm pool. *Climate Dynamics* 33, 565–589, doi:10.1007/s00382-009-0526-7.

Donner, S.D., Skirving, W.J., Little, C.M., Oppenheimer, M., and Hoegh-Guldberg, O. (2005) Global assessment of coral bleaching and required rates of adaptation under climate change. Global Change Biology (2005) 11, 2251–2265, doi: 10.1111/j.1365-2486.2005.01073.x.

Ganachaud, A.S., Sen Gupta, A., Orr, J.C., Wijffels, S.E., Ridgway, K.R., Hemer, M.A., Maes, C., Steinberg, C.R., Tribollet, A.D., Qiu, B., and Kruger, J.C. (2011) Observed and expected changes to the tropical Pacific Ocean. In: J.D. Bell, J.E. Johnson and A.J. Hobday (eds) Vulnerability of Tropical Pacific Fisheries and Aquaculture to Climate Change. Secretariat of the Pacific Community, Noumea, New Caledonia.

Hanley, D.E., Bourassa, M.A., O'Brien, J.J., Smith, S.R. and Spade, E.R. (2003) A Quantitative Evaluation of ENSO Indices. *Journal of Climate*, 16, 1249-1258. https://doi.org/10.1175/1520-0442(2003)16<1249:AQEOEI>2.0.CO;2.

Held, I.M. and Soden, B.J. (2006) Robust responses of the hydrological cycle to global warming: *Journal of Climate*, v. 19, p. 5686-5699. https://doi.org/10.1175/JCLI3990.1.

Huang B., Thorne, P.W., Banzon, V.F., Boyer, T., Chepurin, G., Lawrimore, J.H., Menne, M.J., Smith, T.M., Vose, R.S. and Zhang, H-M. (2017) Extended Reconstructed Sea Surface Temperatures Version 5 (ERSSTv5): Upgrades, Validations, and Intercomparisons. *Journal of Climate*, 30, 8179-8205, https://doi.org/10.1175/JCLI-D-16-0836.1.

Johnson, N.C., Xie, S.P. (2010) Changes in the sea surface temperature threshold for tropical convection: *Nature Geoscience*, v. 3, p. 842-845. DOI: 10.1038/NGEO1008.

Reynolds, R.W., Smith, T.M., Liu, C., Chelton, D.B., Casey, K.S. and Schlax, M.G. (2007) Daily High-Resolution-Blended Analyses for Sea Surface Temperature. *Journal of Climate*, 20, 5473-5496, https://doi.org/10.1175/2007JCLI1824.1.

Rhein, M., Rintoul, S.R., Aoki, S., Campos, E., Chambers, D., Feely, R.A., Gulev, S., Johnson, G.C., Josey, S.A., Kostianoy, A., Mauritzen, C., Roemmich, D., Talley L.D. and Wang, F. (2013) Observations: Ocean. In: Climate Change 2013: The Physical Science Basis. Contribution of Working Group I to the Fifth Assessment Report of the Intergovernmental Panel on Climate Change [Stocker, T.F., D. Qin, G.-K. Plattner, M. Tignor, S.K. Allen, J. Boschung, A. Nauels, Y. Xia, V. Bex and P.M. Midgley (eds.)]. Cambridge University Press, Cambridge, United Kingdom and New York, NY, USA.

Tompkins, A.M. (2001) On the Relationship between Tropical Convection and Sea Surface Temperature. *Journal of Climate*, 14, 633-637, https://doi.org/10.1175/1520-0442(2001)014<0633:OTRBTC>2.0.CO;2.

Waliser, D.E. and Graham, N.E. (1993) Convective Cloud Systems and Warm-Pool Sea Surface Temperatures: Coupled Interactions and Self-Regulation. *Journal of Geophysical Research* 98, 12881-12893. DOI: 10.1029/93JD00872.